Inorg. Chem. **2004**, *43*, 421–429

Dinuclear Complexes of Chiral Tetradentate Pyridylimine Ligands: Diastereoselectivity, Positive Cooperativity, Anion Selectivity, Ligand Self-Sorting Based on Chirality, and Magnetism

Shane G. Telfer,*,† Tomohiro Sato,† Reiko Kuroda,*,†,‡ Julie Lefebvre,§ and Daniel B. Leznoff§

JST ERATO Kuroda Chiromorphology Project, Park Building, 4-7-6 Komaba, Meguro-ku, Tokyo 153-0041, Japan, Graduate School of Arts and Sciences, University of Tokyo, Komaba, Meguro-ku, Tokyo 153-8902, Japan, and Department of Chemistry, Simon Fraser University, 8888 University Drive, Burnaby, BC, Canada V5A 1S6

Received May 29, 2003

The synthesis and coordination chemistry of two chiral tetradentate pyridylimine Schiff base ligands are reported. The ligands were prepared by the nucleophilic displacement of both bromides of 1,3-bis(bromomethyl)benzene (**2**) or 3,5-bis(bromomethyl)toluene (**3**) by the anion of (*S*)-valinol, followed by capping of both amine groups with pyridine-2-carboxaldehyde. Both ligands react with $CoCl_2$ and $NiCl_2$ to give $[M_2L_2Cl_2]^{2+}$ complexes. Remarkably, neither fluoride nor bromide ions can act as bridging ligands. The formation of $[Co_2((S)\text{-}\mathbf{3})_2Cl_2]^{2+}$ is highly diastereoselective, and X-ray crystallography shows that both metal centers in the $[Co_2((S)\text{-}\mathbf{3})_2Cl_2](CoCl_4)$ complex adopt the Λ configuration (crystal data: $[Co_2(C_{31}H_{40}N_4O_2)_2Cl_2](CoCl_4)\cdot(CH_3CN)_3$, monoclinic, $P2_1$, $a = 11.595(2)$ Å, $b = 22.246(4)$ Å, $c = 15.350(2)$ Å, $V = 3705(1)$ Å^3, $\beta = 110.643(3)°$, $Z = 2$). Structurally, the dinuclear complex can be viewed as a helicate with the helical axis running perpendicular to the $[Co_2Cl_2]$ plane. The reaction of racemic **2** with $CoCl_2$ was shown by ^{1}H NMR spectroscopy to yield a racemic mixture of Λ,Λ-$[Co_2((S)\text{-}\mathbf{2})_2Cl_2]^{2+}$ and Δ,Δ-$[Co_2((R)\text{-}\mathbf{2})_2Cl_2]^{2+}$ complexes; that is, a homochiral recognition process takes place. Spectrophotometric titrations were performed by titrating (*S*)-**3** with $Co(ClO_4)_2$ followed by Bu_4NCl, and the global stability constants of $[Co((S)\text{-}\mathbf{3})]^{2+}$ ($\log \beta_{110} = 5.7$), $[Co((S)\text{-}\mathbf{3})_2]^{2+}$ ($\log \beta_{120} = 11.6$), and $[Co_2((S)\text{-}\mathbf{3})_2Cl_2]^{2+}$ ($\log \beta_{110} = 23.8$) were calculated. The results revealed a strong positive cooperativity in the formation of $[Co_2((S)\text{-}\mathbf{3})_2Cl_2]^{2+}$. Variable-temperature magnetic susceptibility curves for $[Co_2((S)\text{-}\mathbf{2})_2Cl_2](BPh_4)_2$ and $[Co_2((S)\text{-}\mathbf{3})_2Cl_2](BPh_4)_2$ are very similar and indicate that there are no significant magnetic interactions between the cobalt(II) centers.

Introduction

Chirality is central to coordination chemistry and unites fields as diverse as transition-metal catalysis, metallosupramolecular chemistry, and bioinorganic chemistry. One research theme which plays a pivotal role in this field is the exploration of methods for the stereoselective synthesis of coordination compounds.[1−3]

We have commenced a research project focusing on ligands derived from chiral amino alcohols. Amino alcohols are ideal building blocks for chiral ligands: a large number of such compounds are readily available in enantiopure form, and naturally the amine and alcohol functionalities can be utilized as donor groups. Our initial investigations have centered on ligands of the general type **1** (Chart 1). These ligands are centered around a benzene core with chiral arms radiating out to Schiff base chelate groups. These arms can be arranged in *ortho*, *meta*, *para*, or 1,3,5 fashion around the benzene core. Two important questions can thereby be systematically addressed: (i) the influence of the relative orientation of the ligand arms on the structure of the metallosupramolecular assembly and (ii) the ability of the chiral centers of the ligand to control the stereochemistry of the metal center(s).

* Author to whom correspondence should be addressed. Fax/phone: +81 3 5465 0104. E-mail: shane.telfer@chiromor2.erato.rcast.u-tokyo.ac.jp.
† JST ERATO Kuroda Chiromorphology Project.
‡ University of Tokyo.
§ Simon Fraser University.

(1) Von Zelewsky, A.; Mamula, O. *J. Chem. Soc., Dalton Trans.* **2000**, 219−231.
(2) Knof, U.; Von Zelewsky, A. *Angew. Chem., Int. Ed.* **1999**, *38*, 303−322.
(3) Provent, C.; Williams, A. F. In *Transition Metals in Supramolecular Chemistry*; Sauvage, J. P., Ed.; John Wiley and Sons: New York, 1999; pp 135−191.

10.1021/ic034585k CCC: $27.50
Published on Web 12/16/2003

Chart 1

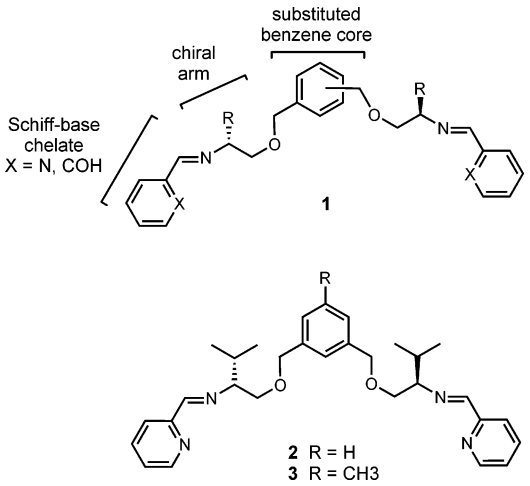

Scheme 1. Synthetic Route to Ligands **2** and **3**

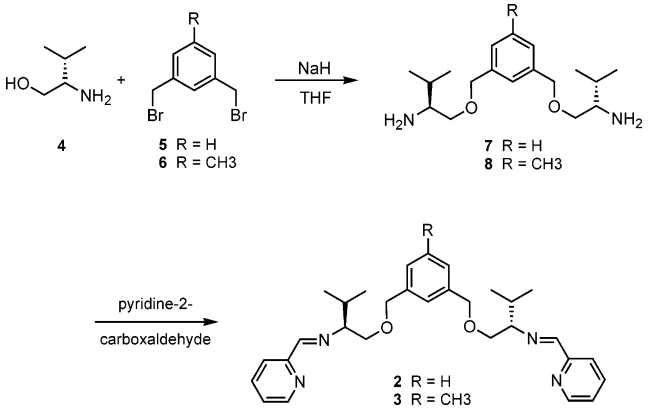

We have recently reported that ligand (*S*)-***2*** forms a dinuclear complex, $[M_2((S)\text{-}\mathbf{2})_2Cl_2]^{2+}$, upon reaction with $CoCl_2$ or $NiCl_2$.[4] The complexation reaction was highly diastereoselective with both metal centers adopting the Λ configuration. However, the CD spectra of these complexes was the inverse of that normally observed for diimine−metal complexes with this stereochemistry. We were able to explain this anomaly by an "internuclear" exciton coupling model whereby coupling between diimine chromophores located on *different* metal centers dominates the observed CD spectrum.[5] Herein we present the full experimental details of this work along with further observations regarding the coordination chemistry of ligands **2** and **3** (Chart 1) including some observations regarding the magnetic and thermodynamic properties of their dinuclear cobalt(II) complexes. It should be noted that we have found that the coordination chemistries of **2** and **3** are very similar, and we have used them interchangeably. Hence, the results described below for a particular ligand can, in general, be equally applied to the other.

Results and Discussion

Synthesis and Coordination Chemistry of 2 and 3. The general synthetic route to ligands **2** and **3** is presented in Scheme 1. The anion of valinol (**4**) was generated by reaction with NaH in THF. Subsequent nucleophilic displacement of the bromides from the appropriate *m*-bis(bromomethyl)arene (**5**) yields compounds **7** and **8**. Thus far we have prepared only these valinolato derivatives. However, this methodology should be suitable for the preparation of other compounds by making use of the large number of commercially available and cheap enantiopure amino alcohols. **7** and **8** are potentially useful synthetic intermediates for a range of bischelating ligands as the amine functionalities can be capped with a range of aldehydes (e.g., salicaldehyde, 2-diphenylphosphinobenzaldehyde). The pyridine-2-carboxaldehyde derivatives (*S*,*S*)-**2** and (*S*,*S*)-**3** (henceforth abbreviated as (*S*)-**2** and (*S*)-**3**) are readily prepared in high yield.

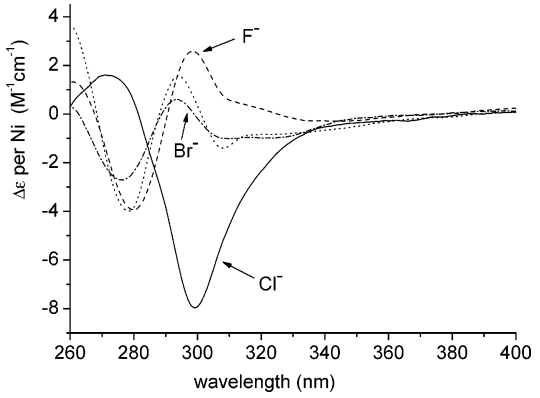

Figure 1. CD spectrum of a 1/1 mixture of $Ni(ClO_4)_2$ and (*S*)-**2** in CH_3CN (···) and following the addition of (a) fluoride ions (---), (b) chloride ions (—), and (c) bromide ions (·-·). These spectra demonstrate a remarkable selectivity for chloride ions in the formation of complexes of the type $\Lambda,\Lambda\text{-}[Ni_2((S)\text{-}\mathbf{2})_2X_2]^{n+}$.

As outlined in our earlier paper, the reaction of (*S*)-**2** with $CoCl_2$ in CH_3CN leads to the dinuclear complex $\Lambda,\Lambda\text{-}[Co_2Cl_2((S)\text{-}\mathbf{2})_2]^{2+}$. This complex can be isolated as either its $CoCl_4^{2-}$ salt or its BPh_4^- salt, and we present the full details of its characterization by ^1H NMR, UV−vis, and CD spectroscopy in the Experimental Section.

We subsequently investigated whether other metal ions and potentially bridging anions (X) would also give rise to complexes of the type $[M_2((S)\text{-}\mathbf{2})_2X_2]^{n+}$. We employed a combinatorial approach whereby a variety of potentially bridging ligands ($X = F^-$, Cl^-, Br^-, OAc^-, SCN^-) were added to separate solutions of 1/1 mixtures of (*S*)-**2** and $M(ClO_4)_2$ salts ($M = Fe^{II}$, Co^{II}, Ni^{II}, Cu^{II}, and Zn^{II}) in CH_3CN. Each sample was then screened for the presence of $[M_2((S)\text{-}\mathbf{2})_2X_2]^{n+}$ complexes by ES-MS and CD spectroscopy (for $X = F^-$, Cl^-, and Br^-).

The only combinations which gave positive "hits" for the presence of $\Lambda,\Lambda\text{-}[M_2((S)\text{-}\mathbf{2})_2X_2]^{n+}$ complexes were the previously investigated Co^{II}/Cl^- and Ni^{II}/Cl^- systems.[4] This demonstrates a remarkable selectivity for chloride ions; neither bromide nor fluoride ions are able to act as bridging ligands. This is clearly illustrated by Figure 1, which shows the CD spectrum of a 1/1 mixture of $Ni(ClO_4)_2$ and (*S*)-**2** along with the spectra measured following the addition of 1 equiv of (a) fluoride ions, (b) chloride ions, and (c) bromide ions. Similar observations were made when the corresponding experiment was performed with cobalt(II) in place of nickel(II).

(4) Telfer, S. G.; Kuroda, R.; Sato, T. *Chem. Commun.* **2003**, 1064−1065.
(5) Telfer, S. G.; Tajima, N.; Kuroda, R. *J. Am. Chem. Soc.*, in press.

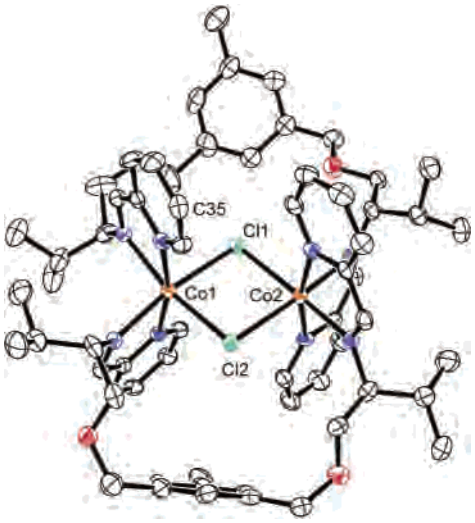

Figure 2. ORTEP plot of the non-hydrogen atoms of the Λ,Λ-$[Co_2((S)\text{-}\mathbf{3})_2Cl_2]^{2+}$ cation. Thermal ellipsoids are shown at the 50% probability level. Key: black = carbon; blue = nitrogen; red = oxygen.

The combination of (*S*)-**2** and iron(II) was found to give $[Fe_2((S)\text{-}\mathbf{2})_3]^{4+}$ or $[Fe((S)\text{-}\mathbf{2})(CH_3CN)_2]^{2+}$ (depending on the Fe/(*S*)-**2** ratio), and these results will be reported in more detail soon.

With respect to the coordination chemistry of (*S*)-**3**, we expected that it would behave in a fashion similar to that of (*S*)-**2** given that the only difference between these ligands is the presence of a methyl substituent on the central aromatic ring. This expectation was borne out by the reaction of (*S*)-**3** with $CoCl_2$, which yielded the dinuclear complex Λ,Λ-$[Co_2((S)\text{-}\mathbf{3})_2Cl_2]^{2+}$. This complex was characterized by ^{1}H NMR spectroscopy, ES-MS, CD spectroscopy, and X-ray crystallography (see below). The ^{1}H NMR spectrum of Λ,Λ-$[Co_2((S)\text{-}\mathbf{3})_2Cl_2]CoCl_4$ displays 13 peaks paramagnetically shifted over a range of about 110 ppm. Analysis of the integrals of these peaks indicates that they account for around 76 of the 80 expected protons for the D_2-symmetric structure. The presence of just one set of peaks indicates that the formation of Λ,Λ-$[Co_2((S)\text{-}\mathbf{3})_2Cl_2]^{2+}$ is highly diastereoselective (de > 95%), as observed for (*S*)-**2**.

The primary motivation for the synthesis of both (*S*)-**2** and (*S*)-**3** was to enable the investigation of ligand exchange reactions between their dinuclear complexes by ES-MS; the different masses of these two ligands would allow differentiation of the three possible $[Co_2((S)\text{-}\mathbf{2})_x((S)\text{-}\mathbf{3})_yCl_2]^{2+}$ complexes. A similar approach has proved fruitful for dinuclear triple helicates.[6] Unfortunately, however, fragmentation of these dinuclear complexes was observed under a range of spectrometer operating conditions. These difficulties precluded a quantitative investigation into the ligand exchange reactions.

X-ray Crystal Structure of Λ,Λ-$[Co_2((S)\text{-}\mathbf{3})_2Cl_2]CoCl_4\cdot(CH_3CN)_3$. The solid-state structure of Λ,Λ-$[Co_2((S)\text{-}\mathbf{3})_2Cl_2]CoCl_4\cdot(CH_3CN)_3$ (Figure 2) is broadly similar to that of the corresponding complex of (*S*)-**2**.[4] The complex cation is centered around a $[Co_2(\mu_2\text{-}Cl)_2]$ core[7,8] which has

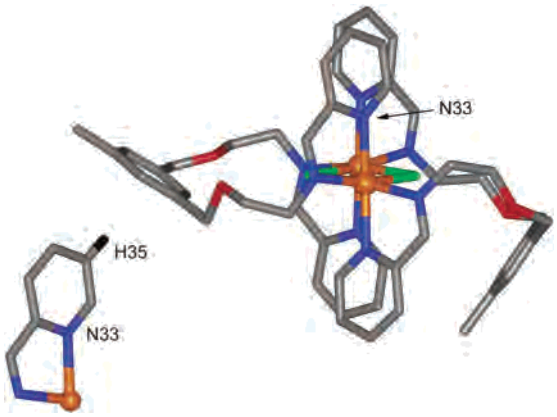

Figure 3. View of the Λ,Λ-$[Co_2((S)\text{-}\mathbf{3})_2Cl_2]^{2+}$ cation down the Co−Co axis emphasizing the orientations of the flexible central aromatic sections of the ligands and the CH−π interaction between the extended aromatic ring and a pyridine ring of a neighboring complex. The isopropyl arms and all hydrogen atoms of the ligands have been removed for clarity. Key: orange = cobalt; green = chloride; gray = carbon; blue = nitrogen; red = oxygen.

a Co···Co separation of 3.66 Å and Co−Cl bond lengths of 2.47−2.48 Å. The two (*S*)-**3** ligands surround this core, spanning the two Co(II) centers in a "side-by-side" manner. An alternative way of viewing the disposition of the ligands is to regard them as forming a double helix, twisting around an axis perpendicular to the $[Co_2(\mu\text{-}Cl)_2]$ core. In this sense, the structure is a right-handed (*P*) helicate.[9] Both Co(II) centers adopt the Λ configuration, and their coordination sphere is somewhat distorted from octahedral. The Co···N bond lengths fall in the range 2.12−2.18 Å. The $[CoCl_4]^{2-}$ counteranion has the expected tetrahedral geometry, and its presence accounts for the intense green color of the crystals.

The orientation of the central aromatic rings of the ligands is an interesting feature of the solid-state structure of Λ,Λ-$[Co_2((S)\text{-}\mathbf{3})_2Cl_2]CoCl_4$. This is highlighted by the side view of the complex in Figure 3. It can be seen that one ring is folded in toward the center of the complex, while the other extends outward from the complex. The rings are thus oriented at an approximate right angle to one another. On the other hand, in Λ,Λ-$[Co_2((S)\text{-}\mathbf{2})_2Cl_2]CoCl_4$ both aromatic rings extend outward from the $[Co_2Cl_2]$ core with a relative angle of 23°.[4]

We can rationalize the observed conformations of the ligands by the following. The central sections of ligands **2** and **3** are rather flexible, and therefore their conformations are likely to be sensitive even to weak intra- or intermolecular interactions. Analysis of the packing of Λ,Λ-$[Co_2((S)\text{-}\mathbf{3})_2Cl_2]\text{-}CoCl_4$ reveals a short contact between the "extended" aromatic ring and a hydrogen atom (H35) of a pyridyl group of a neighboring molecule. The centroid···H distance is 2.54 Å, and the C35−H35 bond makes an angle of 151° with the plane of the aromatic ring. This is strongly suggestive of a stabilizing CH−π interaction and would explain why this

(6) Charbonniere, L. J.; Williams, A. F.; Frey, U.; Merbach, A. E.; Kamalaprija, P.; Schaad, O. *J. Am. Chem. Soc.* **1997**, *119*, 2488−2496.
(7) Shao, C.; Sun, W.-H.; Chen, Y.; Wang, R.; Xi, C. *Inorg. Chem. Commun.* **2002**, *5*, 667−670.
(8) Hemmert, C.; Renz, M.; Gornitzka, H.; Soulet, S.; Meunier, B. *Chem.−Eur. J.* **1999**, *5*, 1766−1774.
(9) For typical helicates, the helical axis is defined as the M−M axis. Piguet, C.; Bernardinelli G.; Hopfgartner G. *Chem. Rev.* **1997**, *97*, 2005−2062.

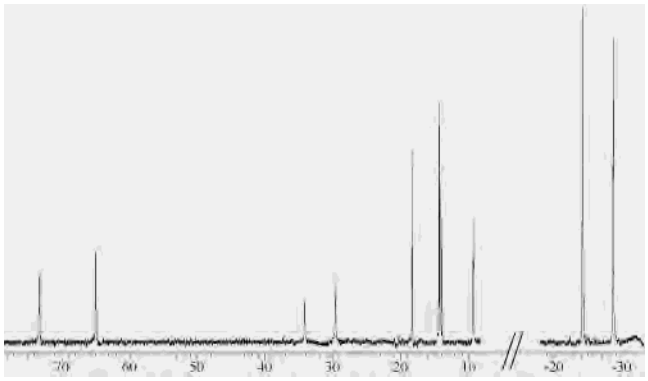

Figure 4. A portion of the ^{1}H NMR spectrum (500 MHz) of *rac*-**2** and $CoCl_2$ (1/1 ratio) in CD_3CN.

aromatic ring extends outward from the core of the complex. Indeed, similar CH$-\pi$ interactions are apparent for *both* ligands in Λ,Λ-$[Co_2((S)\text{-}\mathbf{2})_2Cl_2]CoCl_4$, where *both* ligands are observed to project away form the core of the complex. In the absence of any CH$-\pi$ interactions, the ligand folds inward as seen in Figure 3. This creates a highly nonpolar cavity, and the ether oxygen atoms of the ligand are directed away from this region. Thus, the folding process probably results in free energy gains as a result of favorable hydrophobic interactions. It should be noted that the ^{1}H NMR spectra of both complexes indicate these distortions are lost in solution and the complexes have average D_2 symmetry.

Synthesis of $[Co_2(\mathbf{2})_2Cl_2]^{2+}$ with *rac*-*2*. As outlined above, the reaction of enantiopure (*S*)-**2** with $CoCl_2$ gives Λ,Λ-$[Co_2((S)\text{-}\mathbf{2})_2Cl_2]^{2+}$ as the sole product. We investigated the same reaction with *racemic* **2** by mixing 1 equiv each of (*S*)-**2** and (*R*)-**2** in CD_3CN before adding $CoCl_2$ (1 equiv per total **2**). The ^{1}H NMR spectrum of this solution was recorded, and a set of 12 peaks paramagnetically shifted over a range of around 110 ppm was observed (Figure 4). Tellingly, the spectrum was identical to that observed for Λ,Λ-$[Co_2((S)\text{-}\mathbf{2})_2Cl_2]^{2+}$.

Given that the reaction of $CoCl_2$ with *rac*-**2** also generates $[Co_2(\mathbf{2})_2Cl_2]^{2+}$, there are two distinct pathways the reaction can follow. The first possibility is that the ligands are capable of self/non-self-discrimination (or "social self-sorting"), and a heterochiral complex $[Co_2((S)\text{-}\mathbf{2})((R)\text{-}\mathbf{2})Cl_2]^{2+}$ is formed (eq 1). Alternatively, the ligands may undergo a self−self-recognition process to generate the homochiral complexes Λ,Λ-$[Co_2((S)\text{-}\mathbf{2})_2Cl_2]^{2+}$ and Δ,Δ-$[Co_2((R)\text{-}\mathbf{2})_2Cl_2]^{2+}$ (eq 2). The channeling of these diastereostereomeric processes can be viewed in the broader context of general self-sorting phenomena.[10]

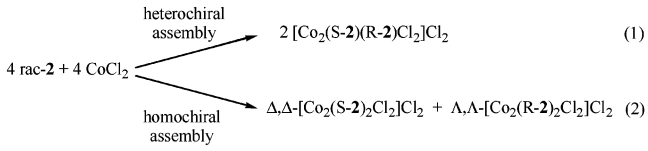

A 1/1 mixture of *rac*-**2** and $CoCl_2$ generates $[Co_2((S)\text{-}\mathbf{2})_2Cl_2]^{2+}$ and $[Co_2((R)\text{-}\mathbf{2})_2Cl_2]^{2+}$. This was demonstrated by the ^{1}H NMR spectrum of this mixture, which was found to be identical to that of $[Co_2((S)\text{-}\mathbf{2})_2Cl_2]^{2+}$. This is likely to be the thermodynamic (rather than kinetic) product distribution given the high lability of the cobalt(II) ion. A plausible explanation for this homochiral self-recognition phenomenon can be gleaned from the X-ray crystal structure of Λ,Λ-$[Co_2((S)\text{-}\mathbf{2})_2Cl_2]^{2+}$ (the core of this complex is structurally identical to that of the (*S*)-**3** complex shown in Figure 2).[4] The four bulky isopropyl substituents of the two ligands are all directed away from the center of the complex and are free from any obvious destabilizing steric interactions. If one of the (*S*)-**2** ligands of Λ,Λ-$[Co_2((S)\text{-}\mathbf{2})_2Cl_2]^{2+}$ is replaced by (*R*)-**2**, however, the isopropyl groups of the (*R*)-**2** ligand would project directly toward the coordinating pyridine rings of the (*S*)-**2** ligand. Thus, if the overall structure of the dinuclear complex is maintained, there is likely to be a significant free energy difference between the homochiral and heterochiral diastereomers which is sufficiently large to steer the reaction down the homochiral pathway.

Both the homochiral[11−13] and heterochiral[14,15] reaction pathways mentioned above have literature precedent for transition-metal complexes, though it remains rather difficult to predict a priori which outcome will be favored. Indeed, structurally similar ligands can display starkly contrasting behavior,[16] and the energy differences can be small enough that mixtures of products are formed.[17,18] There is also at least one reported instance where an entirely new product is formed upon switching from a chiral to a racemic ligand.[14] However, despite these uncertainties, convincing post hoc rationalizations of the observed product distributions can often be made. As in the case reported here, steric effects have often been invoked as being the determining factor.

Thermodynamic Stability Constants. The aim of this section of work was to determine the global stability constant of Λ,Λ-$[Co_2((S)\text{-}\mathbf{3})_2Cl_2]^{2+}$. This was achieved by conducting a series of spectrophotometric titrations which are discussed below. First, however, given that a large number of other $[Co_x((S)\text{-}\mathbf{3})_yCl_z]^{(2x-z)+}$ complexes may also be present at various Co/(*S*)-**3**/Cl^- ratios, careful characterization of these complexes is required for the successful modeling of spectrophotometric data. To this end, ES-MS and ^{1}H NMR titration experiments were performed.

(i) ES-MS and ^{1}H NMR characterization of $[Co_x((S)\text{-}\mathbf{3})_yCl_z]^{(2x-z)+}$ Complexes. A series of ES-MS spectra at differing Co/(*S*)-**3** ratios was obtained by titrating a solution of (*S*)-**3** in CH_3CN with $Co(ClO_4)_2\cdot 6H_2O$. A peak at m/z =

(10) Wu, A.; Isaacs, L. *J. Am. Chem. Soc.* **2003**, *125*, 4831−4835.

(11) Telfer, S. G.; Williams, A. F.; Bernardinelli, G. *Chem. Commun.* **2001**, 1498−1499.
(12) Rowland, J. M.; Olmstead, M. M.; Mascharak, P. K. *Inorg. Chem.* **2002**, *41*, 1545−1549.
(13) Masood, M. A.; Enemark, E. J.; Stack, T. D. P. *Angew. Chem., Int. Ed.* **1998**, *37*, 928−932.
(14) Kim, T. W.; Lah, M. S.; Hong, J.-I. *Chem. Commun.* **2001**, 743−744.
(15) For a related example involving the heterochiral dimerization of M(diimine) complexes, see: Gut, D.; Rudi, A.; Kopilov, J.; Goldberg, I.; Kol, M. *J. Am. Chem. Soc.* **2002**, *124*, 5449−5456.
(16) Provent, C.; Bernardinelli, G.; Williams, A. F.; Vulliermet, N. *Eur. J. Inorg. Chem.* **2001**, 1963−1967.
(17) Amendola, V.; Fabbrizzi, L.; Linati, L.; Mangano, C.; Pallavicini, P.; Pedrazzini, V.; Zema, M. *Chem.—Eur. J.* **1999**, *5*, 3679−3688.
(18) Vincent, J.-M.; Philouze, C.; Pianet, I.; Verlhac, J.-B. *Chem.—Eur. J.* **2000**, *6*, 3595−3599.

530.2 was observed to grow in rapidly at low $Co(ClO_4)_2$/(*S*)-**3** ratios before diminishing at higher ratios. At this point, peaks at $m/z = 279.6$ and 658.2 began to dominate the spectrum. When chloride ions were added, these peaks were gradually replaced by a peak at $m/z = 594.3$.

These observations can be interpreted in a straightforward fashion. Initially $[Co((S)\text{-}\mathbf{3})_2]^{2+}$ ($m/z = 530.2$) is formed. $[Co((S)\text{-}\mathbf{3})]^{2+}$ appears upon the addition of further cobalt(II), as indicated by the steady increase in intensity of the base peak for this complex ($m/z = 279.6$) and its ClO_4^- adduct ($m/z = 658.2$). These $[Co((S)\text{-}\mathbf{3})_x]^{2+}$ ($x = 1, 2$) complexes are subsequently converted into $[Co_2((S)\text{-}\mathbf{3})_2Cl_2]^{2+}$ (m/z 594.3, isotopic peak spacings 0.5 Da) when chloride ions are added. There are a couple of caveats regarding these ES-MS results. First, although the isotope spacings of the peak at $m/z = 594.3$ indicated a 2+ charge (i.e., $[Co_2((S)\text{-}\mathbf{3})_2Cl_2]^{2+}$), we cannot rule out the possibility that the $[Co((S)\text{-}\mathbf{3})Cl]^+$ complex is also present. Second, these complexes are prone to fragmentation under the conditions of ES-MS measurement (as noted above); hence, the observed spectra may not be a full accurate representation of the species present in solution.

A ^{1}H NMR titration was performed in a manner analogous to that of the above ES-MS experiments.[19] As expected, the signals corresponding to free (*S*)-**3** dropped rapidly in intensity when $Co(ClO_4)_2$ was added. However, these were replaced by rather weak and broad paramagnetic peaks, and it was not possible to glean any information from the spectra. We suggest that the ^{1}H NMR signals expected for $[Co((S)\text{-}\mathbf{3})_2]^{2+}$ and $[Co((S)\text{-}\mathbf{3})]^{2+}$ are rendered unobservable by extreme line broadening and/or rapid fluxional processes. A *single* set of peaks corresponding to $[Co_2((S)\text{-}\mathbf{3})_2Cl_2]^{2+}$ was observed when chloride ions were added to the Co/(*S*)-**3** (1/1) solution (Figure S1 in the Supporting Information). Only traces (<5%) of other paramagnetic species were detected.

In summary, the ES-MS experiments imply that $[Co((S)\text{-}\mathbf{3})_2]^{2+}$ is formed rapidly, and $[Co((S)\text{-}\mathbf{3})]^{2+}$ more slowly, when (*S*)-**3** is titrated with $Co(ClO_4)_2$.[20] These complexes are subsequently converted to $[Co_2((S)\text{-}\mathbf{3})_2Cl_2]^{2+}$ in the presence of chloride ions. In conjunction with the ^{1}H NMR experiments, we may tentatively conclude that $[Co_2((S)\text{-}\mathbf{3})_2Cl_2]^{2+}$ is the only species which contains *both* cobalt(II) and chloride ions which is formed in detectable concentrations. However, given the inherent limitations of these techniques, the presence of other such complexes cannot be completely excluded.

(ii) Spectrophotometric Titrations. Spectrophotometric titrations were performed by adding aliquots of $Co(ClO_4)_2 \cdot 6H_2O$ to a solution of (*S*)-**3** in CH_3CN, up to a Co/L ratio of 1/1, followed by the addition of aliquots of Bu_4NCl. The changes to the UV−vis spectrum were monitored in the range 210−450 nm as shown in Figures 5 and 6.

The spectrophotometric data were fitted using the Specfit program.[21,22] A chemical model was devised on the basis of

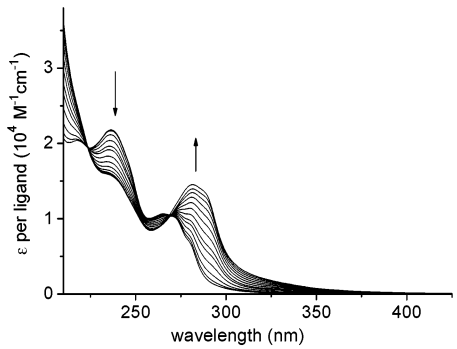

Figure 5. A selection of UV−vis spectra from the spectrophotometric titration of (*S*)-**3** with $Co(ClO_4)\cdot 6H_2O$ in CH_3CN. Co/(*S*)-**3** ratios: free (*S*)-**3**, 0.05, 0.09, 0.16, 0.23, 0.28, 0.36, 0.44, 0.51, 0.59, 0.67, 0.75, 0.97.

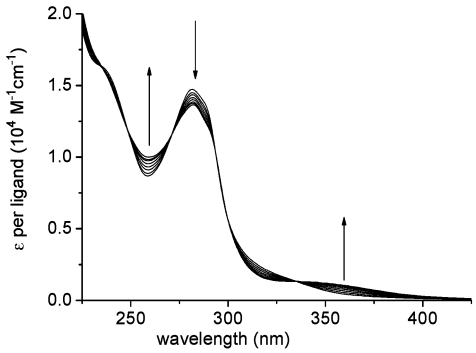

Figure 6. A selection of UV−vis spectra from the spectrophotometric titration of (*S*)-**3**/$Co(ClO_4)\cdot 6H_2O$ (1/1 ratio) with Bu_4NCl in CH_3CN. Cl/(*S*)-**3** ratios: 0.08, 0.23, 0.39, 0.54, 0.69, 0.85, 0.92, 1.08.

Table 1. Global Stability Constants of Cobalt(II) with Ligand (*S*)-**3** and Chloride Ions

$Co + L \rightarrow [CoL]$	$\log \beta_{110} = 5.7(6)$
$Co + 2L \rightarrow [CoL_2]$	$\log \beta_{120} = 11.6(7)$
$2Co + 2L + 2Cl \rightarrow [Co_2Cl_2L_2]$	$\log \beta_{222} = 23.8(9)$

the results of the ES-MS and ^{1}H NMR titrations. $[Co((S)\text{-}\mathbf{3})]^{2+}$ and $[Co((S)\text{-}\mathbf{3})_2]^{2+}$ are clearly important in the first step of the titration ($Co(ClO_4)_2$ added to (*S*)-**3**), and $[Co_2((S)\text{-}\mathbf{3})_2Cl_2]^{2+}$ is certainly formed in the second step (addition of chloride). Thus, a model comprising these three complexes was tested (eqs 3−5),

$$Co^{II} + (S)\text{-}\mathbf{3} \rightleftharpoons [Co(S\text{-}\mathbf{3})]^{2+} \quad (\beta_{110}) \tag{3}$$

$$Co^{II} + 2(S)\text{-}\mathbf{3} \rightleftharpoons [Co(S\text{-}\mathbf{3})_2]^{2+} \quad (\beta_{120}) \tag{4}$$

$$2Co^{II} + 2(S)\text{-}\mathbf{3} + 2Cl^- \rightleftharpoons [Co_2(S\text{-}\mathbf{3})_2Cl_2]^{2+} \quad (\beta_{222}) \tag{5}$$

and an excellent fit with the titration data was obtained. The calculated global stability constants are presented in Table 1. Significantly, the addition of other complexes such as $[Co((S)\text{-}\mathbf{3})Cl]^+$ or $[Co((S)\text{-}\mathbf{3})_2Cl]^+$ to the chemical model dramatically worsened the fit to the data. The absorption spectra predicted by the fitting procedure are chemically reasonable for all complexes, and that of $[Co_2((S)\text{-}\mathbf{3})_2Cl_2]^{2+}$ is

(19) Bu_4NCl was used in place of NH_4Cl for the NMR experiment.
(20) The actual structures of these two complexes remain somewhat uncertain. The coordination sphere of the latter complex may, of course, be completed by solvent molecules.
(21) Gampp, H.; Maeder, M.; Meyer, C. J.; Zuberbuhler, A. D. *Talanta* **1986**, *33*, 943−951.
(22) Specfit/32 for Windows: http://www.bio-logic.fr/rapid-kinetics/specfit/index.html.

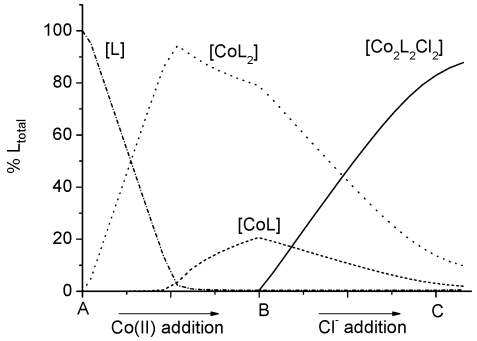

Figure 7. Simulated speciation curves of (*S*)-**3**, $[Co((S)\text{-}\mathbf{3})]^{2+}$, $[Co((S)\text{-}\mathbf{3})_2]^{2+}$, and $[Co_2((S)\text{-}\mathbf{3})_2Cl_2]^{2+}$ during the titration of (*S*)-**3** with $Co(ClO_4)_2\cdot 6H_2O$ (A → B along the *x* axis), followed by Bu_4NCl (B → C along the *x* axis). Point B represents a Co/(*S*)-**3** ratio of 1/1 and point C a Co/(*S*)-**3**/Cl ratio of 1/1/1.

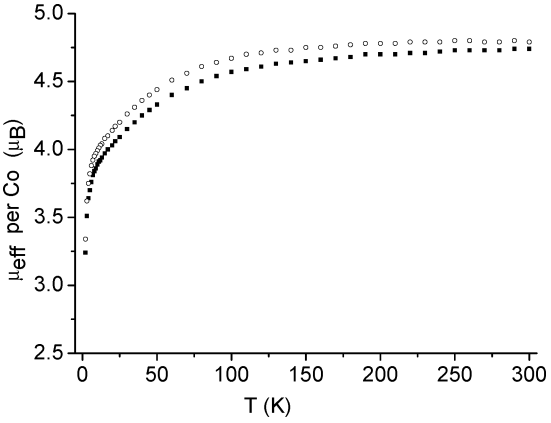

Figure 8. Temperature dependency of the magnetic moment (μ_{eff} per Co center) for $[Co_2((S)\text{-}\mathbf{2})_2Cl_2](BPh_4)_2$ (filled squares) and $[Co_2((S)\text{-}\mathbf{3})_2Cl_2](BPh_4)_2$ (open circles).

in excellent agreement with the spectrum of an isolated sample of the complex (Figure S2 in the Supporting Information).

The concentrations of free (*S*)-**3**, $[Co((S)\text{-}\mathbf{3})]^{2+}$, $[Co((S)\text{-}\mathbf{3})_2]^{2+}$, and $[Co_2((S)\text{-}\mathbf{3})_2Cl_2]^{2+}$ at various stages of the titration were calculated using the stability constants presented in Table 1. The relevant speciation curves are presented in Figure 7. The curves indicate that free (*S*)-**3** is rapidly consumed when cobalt(II) is added. $[Co((S)\text{-}\mathbf{3})_2]^{2+}$ is the dominant complex in the early stages of the titration due to the large excess of ligand which is present. At a Co/(*S*)-**3** ratio of 1/2, this complex accounts for around 95% of the ligand. $[Co((S)\text{-}\mathbf{3})_2]^{2+}$ is gradually replaced by $[Co((S)\text{-}\mathbf{3})]^{2+}$ as the Co/(*S*)-**3** ratio increases; the latter complex accounts for only 20% of the total ligand at a ratio of 1/1.[17] When chloride ions are added to the Co/(*S*)-**3** solution, the concentrations of both of these complexes decline due to the steady formation of $[Co_2((S)\text{-}\mathbf{3})_2Cl_2]^{2+}$.

A second spectrophotometric titration was carried out by adding aliquots of $CoCl_2\cdot 6H_2O$ to a solution of (*S*)-**3** in CH_3CN.[23] In this case, modeling the data with just two complexes—$[Co((S)\text{-}\mathbf{3})_2]^{2+}$ and $[Co_2((S)\text{-}\mathbf{3})_2Cl_2]^{2+}$—provided the best fit. The calculated global stability constants were in accord with those calculated from the first titration; however, the accuracy of these titrations was compromised by the formation of $[CoCl_x]^{(2-x)+}$ species toward $CoCl_2$/(*S*)-**3** ratios of 1/1, which restricted the number of data points available for the fitting procedure. ^{1}H NMR titration results were fully consistent with the chemical model employed in fitting these spectrophotometric data with only one paramagnetic species—$[Co_2((S)\text{-}\mathbf{3})_2Cl_2]^{2+}$—observed at all $CoCl_2$/(*S*)-**3** ratios (Figure S3). Although $[Co((S)\text{-}\mathbf{3})_2]^{2+}$ is invisible by ^{1}H NMR spectroscopy (as discussed above), this complex appears in the ES-MS spectrum at low $CoCl_2$/(*S*)-**3** ratios. Using the stability constants presented in Table 1, a set of speciation curves for the titration of (*S*)-**3** with $CoCl_2$ were simulated (Figure S4).[24] A slow onset to the formation of $[Co_2((S)\text{-}\mathbf{3})_2Cl_2]^{2+}$ is clearly evident; however, this complex becomes the dominant species at $CoCl_2$/(*S*)-**3** ratios greater than 3/4 and is formed almost quantitatively at a 1/1 ratio.

This ensemble of thermodynamic data reveals a strong positive cooperativity in the formation of $[Co_2((S)\text{-}\mathbf{3})_2Cl_2]^{2+}$ when Co(II), (*S*)-**3**, and chloride ions are mixed. That is, the formation of the final structure is thermodynamically favored over every intermediate step along the reaction pathway. Positive cooperativity has been previously observed in the context of metallosupramolecular chemistry, especially for transition-metal helicates.[25−30] With respect to $[Co_2((S)\text{-}\mathbf{3})_2Cl_2]^{2+}$, this cooperative effect is likely to be aided by the chloride bridges of the core of the complex, which will serve to dampen the Coulombic repulsions usually experienced by metal ions when brought close to one another in polynuclear structures.

Magnetic Behavior of the $[Co_2L_2Cl_2]^{2+}$ Complexes. The temperature (*T*) dependencies of the magnetic susceptibility (χ_m) of $[Co_2((S)\text{-}\mathbf{2})_2Cl_2](BPh_4)_2$ and $[Co_2((S)\text{-}\mathbf{3})_2Cl_2](BPh_4)_2$ were measured in the temperature range 2−300 K, and the corresponding graphs of the magnetic moment (μ_{eff} per cobalt atom) as a function of *T* are shown in Figure 8. The complexes show very similar magnetic behavior. At 300 K, μ_{eff} is 4.74 μ_B, consistent with an octahedral, high-spin Co(II) center. Mononuclear octahedral cobalt(II) systems generally have room temperature magnetic moments of 4.7−5.2 μ_B, significantly greater than the spin-only value of 3.87 μ_B due to the large first-order orbital angular momentum contribution to the magnetic moment.[31] The μ_{eff} values are temperature independent until approximately 110 K, below which they drop gradually, reaching 3.24 and 3.34 μ_B for $[Co_2((S)\text{-}\mathbf{2})_2Cl_2](BPh_4)_2$ and $[Co_2((S)\text{-}\mathbf{3})_2Cl_2](BPh_4)_2$ respectively, at 2 K; this drop is likely due primarily to zero-

(23) Titrations were carried out up to a Co(II)/L ratio of 1/1. Beyond this point, formation of $[CoCl_x]^{(2-x)+}$ species became significant.
(24) In reality, we expect the product distribution at high $CoCl_2$/(*S*)-**3** ratios to be slightly more complicated due to the formation of $[CoCl_x]^{(2-x)+}$ species.
(25) Woods, C. R.; Benaglia, M.; Toyota, S.; Hardcastle, K.; Siegel, J. S. *Angew. Chem., Int. Ed.* **2001**, *40*, 749−751.
(26) Glass, T. E. *J. Am. Chem. Soc.* **2000**, *122*, 4522−4523.
(27) Albrecht, M. *Chem. Rev.* **2001**, *101*, 3457−3497.
(28) Hamacek, J.; Blanc, S.; Elhabri, M.; Leize, E.; Dorsselaer, A. V.; Piguet, C.; Albrecht-Gary, A.-M. *J. Am. Chem. Soc.* **2003**, *125*, 1541−1550.
(29) Floquet, S.; Ouali, N.; Bocquet, B.; Bernardinelli, G.; Imbert, D.; Bunzli, J.-C. G.; Hopfgartner, G.; Piguet, C. *Chem.—Eur. J.* **2003**, *9*, 1860−1875.
(30) Pfeil, A.; Lehn, J.-M. *Chem. Commun.* **1992**, 838−840.
(31) Cotton F. A.; Wilkinson G.; Murillo C. A.; Bochmann M. *Advanced Inorganic Chemistry*, 6th ed.; John Wiley & Sons: New York, 1999; p 821.

field splitting effects of the Co(II) centers. Although there may be antiferromagnetic interactions active in these systems, there is no maximum observed in χ_m; hence, any interactions are quite weak (probably <1 cm^{-1}), and we have not attempted to quantify them.[32,33]

These systems, with the absence of any significant magnetic interactions, can be compared to another discrete dinuclear complex with a $[Co^{II}_2(\mu_2\text{-}Cl)_2]$ core for which a very weak antiferromagnetic interaction ($J = -0.63$ cm^{-1}) between the cobalt(II) centers was calculated.[7] The Co···Co distance in this complex is 3.54 Å (compared with 3.54 and 3.66 Å for $[Co_2((S)\text{-}\mathbf{2})_2Cl_2]CoCl_4$ and $[Co_2((S)\text{-}\mathbf{3})_2Cl_2]CoCl_4$, respectively), while the Co−Cl−Co bond angle is 95.8° (average 92.7° and 95.1°, respectively).[34]

In contrast to these weakly coupled systems, $[CoCl_2(4,4'\text{-bipyridine})]_\infty$, a two-dimensional coordination polymer, magnetically orders at 5 K, and chloride-mediated ferromagnetic coupling is a factor in this system.[35] The Co−Cl bond lengths of the polymer are 2.4869(19) Å, while the Co−Co distance is 3.6 Å, and the Co−Cl−Co bond angle is 93.10(9)°. Similarly, ferromagnetic coupling (+5.3 cm^{-1}) was observed in $[Me_3NH]CoCl_3\cdot 2H_2O$, a one-dimensional chain of chloride-bridged octahedral cobalt(II) centers.[36] In this system, the Co−Cl bond lengths are 2.4561(8) and 2.5029(8) Å, while the intrachain Co−Co distance is 3.6366(7) Å; the Co−Cl−Co bond angles are 95.52(4)° and 93.14(4)°.

Metal−ligand bridge angles are known to be important geometric factors in determining the type and strength of magnetic coupling.[37] However, no straightforward correlation between geometry and magnetic interactions can be deduced from the data discussed above. One point which is clear is that the chloride bridges of the $[Co^{II}_2(\mu_2\text{-}Cl)_2]$ moiety are poor mediators of magnetic interactions for the three complexes which have been reported to date. This may arise from a cancellation of ferromagnetic and antiferromagnetic interactions; however, a systematic magnetostructural correlation study for dihalo-bridged octahedral cobalt(II) complexes would be required to examine this point in more detail.

Conclusion

We have introduced a new family of chiral ligands derived from chiral amino alcohols, and in this paper have presented some observations concerning the coordination chemistry of two members of this family. These ligands, (*S*)-***2*** and (*S*)-***3***, were found to react with $CoCl_2$ to give dinuclear complexes $[Co_2L_2Cl_2]^{2+}$ which form with high (>95%) diastereoselectivity; i.e., the chirality of these ligands efficiently predetermines the stereochemistry of the cobalt(II) centers. This chirality is also expressed by homochiral ligand self-sorting when racemic ligand is used to prepare these dinuclear complexes. The formation of $\Lambda,\Lambda\text{-}[Co_2((S)\text{-}\mathbf{3})_2Cl_2]^{2+}$ and $\Lambda,\Lambda\text{-}[Ni_2((S)\text{-}\mathbf{3})_2Cl_2]^{2+}$ is easily monitored by CD spectroscopy, and this method also reveals that neither fluoride nor bromide ions are able to act as bridging ligands. Thermodynamic data derived from spectrophotometric titrations reveal positive cooperativity in the formation of $[Co_2((S)\text{-}\mathbf{3})_2Cl_2]^{2+}$. A wide array of ligands can be constructed from chiral amino alcohols using the methodology presented in this paper, and we anticipate that exploration of their coordination chemistry will continue to deliver many further surprising and enlightening observations.

Experimental Section

General Procedures. ^{1}H NMR spectra were recorded on a JEOL Alpha spectrometer at 500 MHz at 21 °C and referenced to the residual solvent peak (CD_3CN, δ 1.95 ppm; d_6-DMSO, δ 2.50 ppm; $CDCl_3$, δ 7.26 ppm). ^{13}C NMR were recorded at 125 MHz and were reference to the residual solvent peak (CD_3CN, δ 1.32 ppm; d_6-DMSO, δ 36.5 ppm; $CDCl_3$, δ 77.2 ppm). UV−vis absorbance data were recorded using a Shimadzu UV-3150 spectrometer, and extinction coefficients are given in units of M^{-1} cm^{-1}. CD spectra were recorded on a JASCO J720 spectropolarimeter, and $\Delta\epsilon$ values are given in units of M^{-1} cm^{-1}. ES-MS spectra were recorded on a Applied Biosystems Mariner spectrometer with a flow rate of 5 μL/min and at a concentration in the range 10^{-4}−10^{-6} M. Nozzle potentials and temperature (40−50 °C) were kept to a minimum to avoid fragmentation. Microanalyses were performed by Tore Research Centre, Eigiyoo, Tokyo. Unless otherwise stated, chemicals were purchased from Wako, TCI, or Aldrich and used as received. Dried solvents were used for all reactions and measurements.

Preparation of 7. L-Valinol (5.0 g, 48.4 mmol) was dissolved in dry THF (60 mL), and NaH (60% dispersion in mineral oil, 1.94 g, 48.4 mmol) was added in portions with stirring under argon. The solution was then refluxed for 30 min to give a pale yellow suspension and cooled to room temperature, and 1,3-bis(bromomethyl)benzene (4.45 g, 16.9 mmol) was added. The reaction mixture was then refluxed under argon for 16 h and cooled to room temperature, and MeOH (2 mL) was added. The solvent was then removed and the off-white residue partitioned between CH_2Cl_2 and H_2O. The organic layer was separated and extracted with 1 M HCl solution. The aqueous solution was then basified with aqueous NH_3 and extracted with CH_2Cl_2. The organic layer was dried over $MgSO_4$ and the solvent removed to give **7** as a pale yellow oil. Yield: 3.89 g (12.6 mmol, 75%). ^{1}H NMR ($CDCl_3$): δ 0.88−0.90 (m, 12H, CH_3), 1.51 (br s, 4H, NH_2), 1.64 (m, 2H, CH), 2.77 (m, 2H, α-H), 3.28 (dd, 2H, OCH_2CH), 3.50 (dd, 9.5 Hz, 3.5 Hz, 2H, OCH_2CH), 4.50 (AB, $^2J = 12.5$ Hz, 4H, OCH_2Ar), 7.23−7.32 (m, 4H, aromatic H). ^{13}C NMR ($CDCl_3$): δ 18.1, 19.4, 30.9, 56.3, 73.1, 74.0, 126.8 (2C), 128.4, 138.6. ES-MS (CH_3CN, HOAc): $m/z = 309.0$ ([**7**H]$^+$, 100).

Preparation of 8. L-Valinol (1.62 g, 15.7 mmol) was dissolved in dry THF (60 mL), and NaH (60% dispersion in mineral oil, 630 mg, 15.7 mmol) was added in portions with stirring under argon. The solution was then refluxed for 30 min to give a pale yellow suspension and cooled to room temperature, and 3,5-bis(bromomethyl)toluene (1.53 g, 5.5 mmol) was added. The reaction mixture

(32) Sun, J.-S., Zhao, H.; Ouyang, X.; Clerac, R.; Smith, J. A.; Clemente-Juan, J. M.; Gomez-Garcia, C.; Coronado, E.; Dunbar, K. R. *Inorg. Chem.* **1999**, *38*, 5841−5855.
(33) Sakiyama, H.; Ito, R.; Kumagai, H.; Inoue, K.; Sakamoto, M.; Nishida, Y.; Yamasaki, M. *Eur. J. Inorg. Chem.* **2001**, 2027−2032.
(34) The geometric data for our complexes correspond to the X-ray crystal structures which were solved for their $[CoCl_4]^{2-}$ salts, while the magnetic data correspond to their respective BPh_4^- salts.
(35) Lawandy, M. A.; Huang, X.; Wang, R.-J.; Li, J.; Lu, J. Y.; Yuen, T.; Lin, C. L. *Inorg. Chem.* **1999**, *38*, 5410−5414.
(36) Losee, D. B.; McElearney, J. N.; Shankle, G. E.; Carlin, R. L.; Cresswell, P. J.; Robinson, W. T. *Phys. Rev. B* **1973**, *8*, 2185.
(37) Willet, R. D., Gatteschi, D., Kahn, O., Eds. *Magneto-structural Correlations in Exchange Coupled Systems*; Reidel: Dordrecht, The Netherlands, 1985.

was then refluxed under argon for 16 h and cooled to room temperature, and H_2O (2 mL) was added. The THF was then removed and the off-white residue partitioned between CH_2Cl_2 and H_2O. The organic layer was separated and extracted with 1 M HCl solution. The aqueous solution was then basified with aqueous NH_3 and extracted with CH_2Cl_2. The organic layer was dried over $MgSO_4$ and the solvent removed to give a pale yellow oil. Yield: 1.50 g (4.7 mmol, 85%). ^{1}H NMR ($CDCl_3$): δ 0.91−0.93 (m, 12H, CH_3), 1.63−1.70 (br m, 6H, CH and NH_2), 2.35 (s, 3H, ArCH_3), 2.79 (m, 2H, α-H), 3.30 (dd, 2H, OCH_2CH), 3.52 (dd, 2H, OCH_2CH), 4.48 (AB, 4H, OCH_2Ar), 7.08 (s, 2H), 7.11 (s, 1H). ^{13}C NMR ($CDCl_3$): δ 18.3, 19.6, 21.5, 31.0, 56.5, 73.4, 74.2, 124.3, 127.9, 138.4, 138.7. ES-MS (CH_3CN, HOAc): m/z = 323.2 ([**8**H]$^+$, 100), 161.1 ([**8**H$_2$]$^{2+}$, 36).

Preparation of 2. Amine **7** (0.50 g, 1.62 mmol) was taken up in dry MeOH (10 mL), and pyridine-2-carboxaldehyde (0.347 g, 3.24 mmol) was added. Molecular sieves (4 Å) were added, and the solution was stirred overnight under argon. The solvent was removed under reduced pressure and the yellow-brown oily residue analyzed by ^{1}H NMR. If any starting material was present, the product was purified by chromatography on alumina using CH_2Cl_2/MeOH (98/2) as the eluent. Yield: in the range 85−100%. ^{1}H NMR ($CDCl_3$): δ 0.88−0.91 (m, 12H, CH_3), 2.03 (m, obscured by solvent peak, CH), 3.23 (m, 2H, α-H), 3.56 and 3.69 (ABX, 4H, OCH_2CH), 4.43 (m, 4H, OCH_2Ar), 7.15 (m, 4H), 7.29 (m, 2H, pyridyl), 7.72 (m, 2H, pyridyl), 8.01 (d, 2H, pyridyl), 8.34 (s, 2H, imine H), 8.63 (d, 2H, pyridyl). ^{13}C NMR ($CDCl_3$): δ 18.8, 201, 30.4, 72.1, 73.1, 76.9, 121.6, 124.7, 126.8 (2C), 128.5, 136.6, 138.7, 149.5, 154.9, 162.1. ES-MS (CH_3CN, HOAc): m/z = 487.0 ([**2**H]$^+$, 100). UV−vis (CH_3CN): λ_{max} 271 nm (ϵ 10800), 236 nm (23150). CD (CH_3CN): λ_{max} 329 nm ($\Delta\epsilon$ −0.060), 287 nm (0.12), 268 nm (−0.79).

Preparation of 3. Compound **3** was prepared in the same manner as **2**. Yield: in the range 85−100%. ^{1}H NMR ($CDCl_3$): δ 0.86−0.92 (m, 12H, CH_3), 2.00 (m, 2H, CH), 2.21 (s, 3H, ArCH_3), 3.23 (m, 2H, α-H), 3.56 and 3.70 (ABX, 4H, OCH_2CH), 4.38 and 4.42 (AB, 4H, OCH_2Ar), 7.25 (m, 3H), 7.29 (m, 2H, pyridyl), 7.71 (m, 2H, pyridyl), 8.02 (d, 2H, pyridyl), 8.34 (s, 2H, imine), 8.63 (d, 2H, pyridyl). ^{13}C NMR ($CDCl_3$): δ 19.1, 20.3, 30.6, 32.0, 72.3, 73.4, 76.7, 121.9, 124.3, 125.0, 127.9, 136.9, 138.4, 138.8, 149.8, 155.2, 162.4. ES-MS (CH_3CN, HOAc): m/z = 501.0 ([**3**H]$^+$, 100). UV−vis (CH_3CN): λ_{max} 271 nm (sh, ϵ 10250), 265 nm (10600), 237 nm (21700). CD (CH_3CN): λ_{max} 233 ($\Delta\epsilon$ 13.5), 268 nm (−1.7).

Preparation of [Co$_2$(L)$_2$Cl$_2$](CoCl$_4$) Complexes. (i) General Notes. It was found that equimolar mixture of reagents ($CoCl_2$ and ligand) led to the best yield of the [Co$_2$(L)$_2$Cl$_2$](CoCl$_4$) complexes despite this ratio not matching the stoichiometry of the product. We believe that this is due to the formation of other species at $CoCl_2$/L ratios greater than 1/1. This is consistent with the observation that solutions of dissolved crystals of the [Co$_2$(L)$_2$Cl$_2$]-(CoCl$_4$) complexes were not stable over long periods of time. We did not pursue this point in detail as precipitation of the complex cations with $NaBPh_4$ (see below) was found to be a superior synthetic route, and the resulting BPh_4^- salts are stable over long periods in solution.

(ii) [Co$_2$((*S*)-2)$_2$Cl$_2$]CoCl$_4$. In a typical procedure, $CoCl_2 \cdot 6H_2O$ (0.5 mmol) and (*S*)-**2** (0.5 mmol) were combined in CH_3CN (1.5 mL) and diethyl ether (4 mL) was added to give a thick green oil. The brown supernatant was removed and the remaining dark green oil washed with ether. A minimum amount of hot CH_3CN was then added to dissolve the oil and the solution cooled to give a green crystalline precipitate which was filtered off, washed with ether, and dried under vacuum. Yield: ca. 60% (based on $CoCl_2$). ^{1}H NMR (CD_3CN, approximate integrals given): δ −28.74 (12H), −24.22 (12H), 1.28 (4H), 4.59 (8H), 9.29 (6H), 13.91 (4H), 14.36 (4H), 18.40 (4H), 29.28 (4H), 34.56 (2H), 65.00 (4H), 73.34 (4H). UV−vis (CH_3CN, 10^{-4} M): λ_{max} 283 nm (ϵ 26300). CD (CH_3CN, 10^{-4} M): λ_{max} 293 nm ($\Delta\epsilon$ −30.0), 267 nm (6.22). Anal. Calcd (Found) for [Co$_2$((*S*)-**2**)$_2$Cl$_2$]CoCl$_4$·2H$_2$O ($C_{60}H_{84}Cl_6Co_3N_8O_6$): C, 51.37 (51.0); H, 6.04 (5.8); N, 7.99 (7.7).

(iii) [Co$_2$((*S*)-3)$_2$Cl$_2$](CoCl$_4$). This complex was prepared in a manner similar to that of the above complex. ^{1}H NMR (CD_3CN, approximate integrals given): δ −28.42 (12H), −24.21 (12H), 1.06 (4H), 4.82 (8H), 7.53 (8H), 9.37 (6H), 14.16 (4H), 14.37 (4H), 18.17 (4H), 29.28 (4H), 34.56 (2H), 64.43 (4H), 73.02 (4H). UV−vis (CH_3CN, 10^{-4} M): λ_{max} 282 nm (ϵ 34200). CD (CH_3CN, 10^{-4} M): λ_{max} 293 nm ($\Delta\epsilon$ −31.1), 267 nm (5.68). ES-MS (CH_3NO_2): m/z = 594.2 ([M]$^{2+}$, 100). Anal. Calcd (Found) for [Co$_2$((*S*)-**3**)$_2$Cl$_2$]-(CoCl$_4$)·H$_2$O ($C_{62}H_{82}Cl_6Co_3N_8O_5$): C, 52.85 (53.3); H, 5.87 (6.4); N, 7.95 (7.6).

Preparation of [Co$_2$(L)$_2$Cl$_2$](BPh$_4$)$_2$ Complexes (L = 2, 3). A sample of the appropriate ligand (**2** or **3**, 0.15 mmol) was dissolved in dry MeOH (1 mL), and a solution of $CoCl_2 \cdot 6H_2O$ (35.7 mg, 0.15 mmol) in MeOH was added to give a red solution. A solution of $NaBPh_4$ (117 mg, 2.2 equiv) in MeOH (2 mL) was then added with rapid stirring. A pale orange precipitate formed which was filtered off, washed with MeOH and diethyl ether, and air-dried. Yield: 85%.

(i) [Co$_2$((*S*)-2)$_2$Cl$_2$](BPh$_4$)$_2$. ^{1}H NMR (CD_3NO_2, approximate integrals given): δ −27.95 (12H) and −25.06 (12H), 0−10 obscured by H_2O, solvent, and BPh_4^-, 13.61−14.29 (m, 8H), 19.44 (4H), 30.31 (4H), 33.87 (2H), 66.89 (4H), 75.07 (4H). ES-MS (CH_3NO_2): m/z = 580.2 ([M]$^{2+}$, 100). UV−vis (CH_3CN, 10^{-4} M): λ_{max} 275 nm (ϵ 26500). CD (CH_3CN, 10^{-4} M): λ_{max} 293 nm ($\Delta\epsilon$ −25.4), 267 nm (7.50). Anal. Calcd (Found) for [Co$_2$((*S*)-**2**)$_2$Cl$_2$]-(BPh$_4$)$_2$·3H$_2$O·CH$_3$OH ($C_{109}H_{126}B_2Cl_2Co_2N_8O_8$): C, 69.39 (69.5); H, 6.73 (6.4); N, 5.94 (5.3).

(ii) [Co$_2$((*S*)-3)$_2$Cl$_2$](BPh$_4$)$_2$. ^{1}H NMR (CD_3CN, approximate integrals given): δ −28.80 (12H), −24.31 (12H), 4.73 (4H), 6.94−7.69 (BPh$_4$), 9.37 (4H), 14.21 (6H), 14.59 (4H), 18.27 (4H), 19.9 (2H), 29.10 (4H), 34.73 (2H), 64.83 (4H), 73.45 (4H). UV−vis (CH_3CN, 10^{-4} M): λ_{max} 276 nm (ϵ 26000). CD (CH_3CN, 10^{-4} M): λ_{max} 293 nm ($\Delta\epsilon$ −26.2), 267 nm (6.95). ES-MS (CH_3NO_2): m/z = 594.2 ([M]$^{2+}$, 100). Anal. Calcd (Found) for [Co$_2$((*S*)-**3**)$_2$Cl$_2$]-(BPh$_4$)$_2$·H$_2$O ($C_{110}H_{122}B_2Cl_2Co_2N_8O_5$) = C, 71.55 (71.2); H, 6.66 (6.7); N, 6.07 (5.5).

Preparation of [Co$_2$(2)$_2$Cl$_2$]$^{2+}$ with Racemic Ligand. A solution of $CoCl_2 \cdot 6H_2O$ (2.55 mg, 10.7 μmol) in CD_3CN (300 μL) was added to a solution of (*S*)-**2** (2.60 mg, 5.35 μmol) and (*R*)-**2** (2.60 mg, 5.35 μmol) in CD_3CN (300 μL).

ES-MS Titrations. A solution of Co(ClO$_4$)$_2$·6H$_2$O in CH_3CN (ca. 10^{-2} M) was added in eight aliquots to a solution of (*S*)-**3** in CH_3CN (ca. 3×10^{-6} M). A solution of NH_4Cl in methanol (0.07 M) was then added in eight aliquots. ES-MS spectra were recorded after each addition.

^{1}H NMR Titrations. (i) Procedure 1. A solution of $CoClO_4 \cdot 6H_2O$ in CD_3CN was added in aliquots to a solution of (*S*)-**3** in CD_3CN (ca. 10^{-2} M) to give a final Co/(*S*)-**3** ratio of 1/1. A solution of Bu_4NCl in CD_3CN was then added in aliquots to give a final Co/(*S*)-**3** ratio of 1/1/. The ^{1}H NMR spectrum was recorded following the addition of each aliquot.

(ii) Procedure 2. A solution of $CoCl_2 \cdot 6H_2O$ in CD_3CN was added in aliquots to a solution of (*S*)-**3** in CD_3CN (ca. 10^{-2} M) to give a final $CoCl_2$/(*S*)-**3** ratio of 1/1. The ^{1}H NMR spectrum was recorded following the addition of each aliquot.

Spectrophotometric Titrations. All operations were performed at 21.5 °C in a controlled-temperature environment using the UV−vis instrumentation described above. Data were analyzed with the Specfit program.[19,21] Titrations were performed to obtain three stability constants which agreed with each other within the error limits estimated by the software. The averaged values are presented in Table 1.

(i) Procedure 1. A solution of $CoClO_4 \cdot 6H_2O$ in CH_3CN (ca. 3×10^{-2} M) was added in aliquots to a solution of ligand **3** in CH_3CN (ca. 1×10^{-5} M) to give a Co/**3** ratio of 1/1. A solution of Bu_4NCl in CH_3CN (ca. 5×10^{-3} M) was then titrated in to give a Co/**3**/Cl ratio of 1/1/1.2. The UV−vis spectrum was recorded following the addition of each aliquot.

(ii) Procedure 2. A solution of $CoCl_2 \cdot 6H_2O$ in CH_3CN (ca. 3×10^{-2} M) was added in aliquots to a solution of (*S*)-**3** in CH_3CN (ca. 1×10^{-5} M)) to give a final $CoCl_2$/(*S*)-**3** ratio of 1/1. The UV−vis spectrum was recorded following the addition of each aliquot.

Magnetic Measurements. Variable-temperature magnetic susceptibility data were collected using a Quantum Design SQUID MPMS-5S magnetometer working down to 2 K at a 1 T field strength. All data were corrected for TIP, the diamagnetism of the PVC sample holder, and the constituent atoms (by use of Pascal constants).[38]

Crystal Data for $[Co_2(C_{31}H_{40}N_4O_2)_2Cl_2](CoCl_4) \cdot (CH_3CN)_3$. Dark green triangular crystals grew over a period of two weeks at room temperature from a solution of $CoCl_2 \cdot 6H_2O$ and (*S*)-***3*** in CH_3CN. Crysal data: monoclinic, $P2_1$, $a = 11.595(2)$ Å, $b = 22.246(4)$ Å, $c = 15.350(2)$ Å, $V = 3705\ (1)$ Å^3, $\beta = 110.643(3)°$, $Z = 2$, $D_{calcd} = 1.357$ g cm^{-3}. A total of 27513 reflections were collected using a Bruker APEX system at 110 K with Mo Kα radiation. A total of 15744 unique reflections ($R_{int} = 0.050$) were collected. Data were corrected for Lorentzian and polarization. No absorption correction was applied due to crystal decay. The structure was solved by direct methods, and refined against $|F|^2$ using anisotropic thermal displacement parameters for all non-hydrogen atoms (isotropic for the disordered ether oxygen atoms mentioned below). Hydrogen atoms were placed in calculated positions. One of the ether oxygen atoms displayed a large thermal displacement parameter which was modeled as a disorder over two sites with a 0.74/0.26 occupation ratio. The final *R* factor for 11119 reflections ($I > 2\sigma I$) with 789 variables was 0.048 ($R_w = 0.102$), and the absolute structure parameter was −0.01(1). Residual electron density peaks: min −0.49, max 0.88 e Å^{-3}. Calculations used the SHELXL76 program. The ORTEP plot was made using ORTEP-3.[39]

Acknowledgment. S.G.T. thanks the JSPS for the provision of a postdoctoral fellowship. D.B.L. thanks NSERC of Canada for financial support.

Supporting Information Available: ^{1}H NMR spectra from the titration of (*S*)-**3**/$Co(ClO_4)_2$ (1/1 ratio) with Bu_4NCl (Figure S1), a comparison of measured and predicted absorption spectra of $[Co_2((S)\text{-}\mathbf{3})_2Cl_2]^{2+}$ (Figure S2), ^{1}H NMR spectra from the titration of (*S*)-**3** with $CoCl_2$ (Figure S3), speciation curves for the titration of (*S*)-**3** with $CoCl_2$ (Figure S4), and crystallographic data in CIF format. This material is available free of charge via the Internet at http://pubs.acs.org.

IC034585K

(38) Kahn, O. *Molecular Magnetism*; VCH: Weinheim, Germany, 1993.

(39) Farrugia, L. J. *J. Appl. Crystallogr.* **1997**, *30*, 565.